AGU PUBLICATIONS

JGR

Journal of Geophysical Research: Oceans

RESEARCH ARTICLE

10.1002/2014JC009828

Key Points:
- We model circulation and thermal structure in Saginaw Bay and Lake Huron
- New estimates for residence times and exchange between the bay and the main lake
- Estimated diffusivities using Lagrangian drifters and particle transport models

Correspondence to:
M. S. Phanikumar,
phani@egr.msu.edu

Citation:
Nguyen, T. D., P. Thupaki, E. J. Anderson, and M. S. Phanikumar (2014), Summer circulation and exchange in the Saginaw Bay-Lake Huron system, *J. Geophys. Res. Oceans*, *119*, 2713–2734, doi:10.1002/2014JC009828.

Received 17 JAN 2014
Accepted 31 MAR 2014
Accepted article online 8 APR 2014
Published online 29 APR 2014

Summer circulation and exchange in the Saginaw Bay-Lake Huron system

Tuan D. Nguyen[1], Pramod Thupaki[1,2], Eric J. Anderson[3], and Mantha S. Phanikumar[1]

[1]Departmentof Civil and Environmental Engineering, Michigan State University, East Lansing, Michigan, USA, [2]Institute of Ocean Sciences, Fisheries and Oceans Canada, Sidney, British Columbia, Canada, [3]NOAA Great Lakes Environmental Research Laboratory, Ann Arbor, Michigan, USA

Abstract We use a three-dimensional, unstructured grid hydrodynamic model to examine circulation and exchange in the Saginaw Bay-Lake Huron system during the summer months for three consecutive years (2009–2011). The model was tested against ADCP observations of currents, data from a Lagrangian drifter experiment in the Saginaw Bay, and temperature data from the National Data Buoy Center stations. Mean circulation was predominantly cyclonic in the main basin of Lake Huron with current speeds in the surface layer being highest in August. Circulation in the Saginaw Bay was characterized by the presence of an anticyclonic gyre at the mouth of the outer bay and two recirculating cells within the inner bay. New estimates are provided for the mean flushing times (computed as the volume of the bay divided by the rate of inflow) and residence times (computed as *e*-folding flushing times based on dye concentration modeling treating the bay as a continuously stirred tank reactor) for Saginaw Bay. The average flushing time (over the 3 months of summer and for all 3 years) was 23.0 days for the inner bay and 9.9 days for the entire bay. The mean *e*-folding flushing time was 62 days (2 months) for the inner bay and 115 days (3.7 months) for the entire bay for the summer conditions examined in this work. To characterize the behavior of river plumes in the inner Saginaw Bay, trajectory data from GPS-enabled Lagrangian drifters were used to compute the absolute diffusivity values in the alongshore and cross-shore directions.

1. Introduction

The Saginaw Bay-Lake Huron system is significantly impacted by human activities and figures prominently in the list of Areas of Concern (Great Lakes Water Quality Agreement, 1978). Persistent contamination of the water column and bottom sediment has resulted in degraded water quality. It is well known that embayed regions tend to accumulate contaminants due to their long residence times [*Nixon et al*., 1996]. Offshore transport and mixing with lake waters are the dominant processes responsible for the reduction of contaminant concentrations in embayed regions attached to large lakes [*Ge et al*., 2012; *Thupaki et al*., 2010]. While mixing is dominated by small-scale hydrodynamics and shear [*Lawrence et al*., 1995; *Spydell et al*., 2007], advective exchange between Saginaw Bay and Lake Huron is strongly influenced by large-scale circulation patterns.

The large-scale circulation in Lake Huron was first described by *Harrington* [1894], who used data from drift bottle studies to conclude that circulation pattern is generally counterclockwise in the main basin of Lake Huron. While drift bottles have higher error than modern Lagrangian drifter designs due to stokes drift, wind forces, and lack of real-time GPS tracking, many of the conclusions Harrington arrived at have since then been supported by later observations. *Sloss and Saylor* [1976] used observational data sets from extensive current mooring measurements to confirm that while the northern two thirds of the lake is dominated by counterclockwise circulation during summer, the shallower southern part shows a much more complex circulation pattern. They also found that stratification during summer allowed the inertial component to dominate open lake circulation.

Circulation in Lake Huron shows more spatial variation than the other large lakes of comparable size in North America (e.g., Lake Superior and Lake Michigan) due to the presence of several islands, bays, and other complex physical features. In Saginaw Bay, physical features including shallow depths and the presence of a sill near the entrance of the Bay City Basin (BCB) produce a complex circulation pattern. As a result, hydrodynamic models using coarse grids will not be able to adequately resolve circulation within the

© 2014. American Geophysical Union. All Rights Reserved.

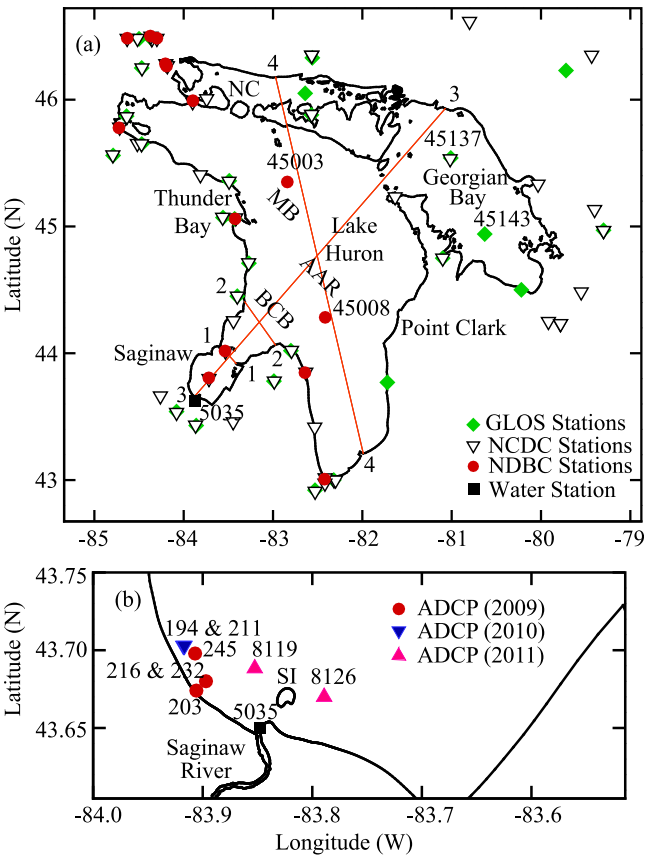

Figure 1. (a) Map of Lake Huron showing the important physical features. MB: Manitoulin Basin, BCB: Bay City Basin, NC: North Channel, AAR: Alpena-Amberley Ridge; (b) Saginaw Bay showing the ADCP locations. SI: Shelter Island. 1-1 and 2-2 in Figure 1a are the inner and outer Saginaw Bay transects, respectively, and 3-3 and 4-4 are transects for which vertical temperature profiles are shown.

Saginaw Bay. Lake Huron has four distinct basins as shown in Figure 1a, with several islands (St. Joseph Island, Bois Blanc Island, Drummond Island, Cockburn Island, Clapperton Island, Manitoulin Island, Fitzwilliam Island, Charity Island, etc.) and bays (Georgian Bay, Saginaw Bay, and Thunder Bay). The prominent bathymetric feature in Lake Huron is the midlake ridge that extends southeastward from Thunder Bay at Alpena on the west side across to Point Clark on the east side. The ridge (Alpena-Amberley Ridge (AAR)) separates the lake into the southwestern and northeastern basins. The shallower southwestern basin has a maximum depth of about 90 m while the deeper northeastern basin has a maximum depth of about 200 m. Accurately representing the physical features of the lake basin in the computational domain is necessary in order to simulate currents, thermal structure, as well as large-scale hydrodynamics. Studies using numerical models to examine circulation in Lake Huron have used multiresolution (nested) structured grids [*Sheng and Rao*, 2006] or coarse-resolution unstructured grids [*Bai et al*., 2013]. In order to reduce the numerical error in simulating the thermocline and horizontal pressure gradient terms, *Sheng and Rao* [2006] used the *z*-level ocean model (CANDIE) [*Sheng et al*., 1998]. *Bai et al*. [2013] used the σ-coordinate, unstructured grid ocean model (GL-FVCOM), which is based on the FVCOM originally developed by *Chen et al*. [2003], and implemented in all five Great Lakes with 21 terrain following σ-layers in the vertical to simulate circulation and thermal structure for the period 1993–2008. Recently, *Anderson and Schwab* [2013] used the unstructured grid Finite Volume Coastal Ocean Model (FVCOM) to develop a Lake Michigan-Huron model to simulate currents in the Straits of Mackinac. In this study, we have used the unstructured grid FVCOM model with grid nesting implemented for the Saginaw Bay region of interest.

Saginaw Bay is an important part of Lake Huron that receives flow from the Saginaw River. The Bay is 87 km long, and the width varies between 20 km and 46 km. The Bay is often divided into the inner and outer regions based on topographic features (Figure 1a). The Saginaw River, which drains an area of over 16,000 km^2, is the major source to the Bay with an average discharge of about 100 m^3/s [*Danek and Saylor*, 1977]. Using time series analyses and numerical simulations, *Allender* [1975] and *Allender and Green* [1976] determined that circulation within the bay is coupled to large-scale circulation in Lake Huron. Using a combination of Lagrangian drifter observations from current meters deployed in Saginaw Bay, *Danek and Saylor* [1977] and *Saylor and Danek* [1976] determined the circulation patterns inside Saginaw Bay for different wind directions. They found that when wind direction was parallel to the axis of the bay, the exchange rate between the inner and outer bays was 3700 m^3/s. More recently, in their analysis of the seasonal circulation in the Great Lakes, *Beletsky et al*. [1999] observed that mean currents during winter are higher than during summer months. Based on the surface current measurements, they also inferred the presence of a return

© 2014. American Geophysical Union. All Rights Reserved.

flow out of Georgian Bay at deeper depths. *Schertzer et al*. [2008] have compiled the mean circulation, inter-lake exchange, and climatology for Lake Huron.

Results based on dye diffusion studies in open lakes and oceans indicate that while mixing rates in open waters follow the Okubo 4/3 power-law scaling [*Okubo*, 1971], mixing rates close to shore are higher due to shear effects resulting from lateral and bottom boundaries [*Lawrence et al*., 1995; *Peeters et al*., 1996; *Stocker and Imberger*, 2003; *Ojo et al*., 2006; *Thupaki et al*., 2013]. Based on data from a continuous Rhodamine-WT dye release study conducted during summer 2008, *Thupaki et al*. [2013] estimated a mean horizontal dispersion coefficient of about 5.6 m^2/s close to the shore in southern Lake Michigan. Dispersion rates in the nearshore can also be calculated using Lagrangian drifters, which have the advantage of higher sampling rate [*Spydell et al*., 2007; *Nekouee*, 2010]. *Spydell et al*. [2007] calculated the absolute (one-particle) dispersion (κ_{xx}, κ_{yy}) and relative (two-particle) dispersion (D_{xx}, D_{yy}) rates using statistical analyses of drifter observations. They found that the relative diffusion rate (D) for Lagrangian particles followed the scaling ($D \sim l^{2/3}$) in the surf-zone, where l is the particle separation distance. *Brown et al*. [2009] found that rates are higher in the presence of rip currents with relative diffusion rates following the relation ($D \sim l^{1/5}$) on rip-channel beaches. In the presence of sheared alongshore currents, *Spydell et al*. [2009] found that alongshore diffusivity is greater than cross-shore diffusivity, but still lower than the diffusion rate predicted for 2D inertial subrange ($D \sim l^{4/3}$). Absolute diffusion rates can also be calculated from single-point Lagrangian drifter statistics by assuming isotropic turbulence. Using particle diffusion trajectories in the surf-zone, *Spydell et al*. [2007] found that diffusion rates in the alongshore and cross-shore directions varied from 4.5 m^2/s to 0.7 m^2/s over a 2 day period.

First-order transport timescales such as residence times and flushing times within the bay are useful for understanding and interpreting the fate and transport of contaminants, nutrient budgets, and the occurrence of harmful algal blooms, and for comparing processes and rates across different ecosystems [*Monsen et al*., 2002]. Significant progress has been made in recent years in characterizing the transport timescales for surface water bodies using hydrodynamic and transport models [*Andutta et al*., 2013; *Camacho and Martin*, 2012; *Phelps et al*., 2013; *Hsu et al*., 2013; *Wan et al*., 2013; *Liu et al*., 2012; *Andradóttir et al*., 2012; *Jouon et al*., 2006]. Although some estimates of residence times are available for the Saginaw Bay [*Dolan*, 1975; *Saylor and Danek*, 1976], they are nearly 40 years old and much has changed in terms of our ability to observe and model natural systems since then. Recent concerns associated with environmental issues in the Saginaw Bay highlight the need for accurate estimates of transport timescales in the bay and one of the objectives of this work is to fill this gap. Terms such as residence time and flushing time, however, are defined and used in many different ways in the literature. Following the suggestions of *Monsen et al*. [2002] and *Bolin and Rodhe* [1973] who recommend that the terms be defined precisely and used with care to avoid confusion, we define these transport timescales in the next section and describe how they are calculated. The aim of this study, therefore, was to characterize circulation and thermal structure in Lake Huron and Saginaw Bay during the summer months using a high-resolution unstructured grid numerical model (FVCOM) and to provide new estimates for the volumetric flux of water exchanged between Saginaw Bay and Lake Huron. Model results are compared against ADCP measurements during the summer months for three consecutive years (2009, 2010, and 2011). The results from the numerical model are then used to calculate volumetric exchange rates for both the inner and outer Saginaw Bay and to estimate first-order transport timescales such as the residence time/flushing time and to examine their interannual variability. Using data from a Lagrangian drifter release conducted near the mouth of Saginaw River, we also calculate absolute particle diffusion rates within the inner Saginaw Bay near the mouth of the Saginaw River.

2. Methods

Current velocity profiles were measured during the summer months of 2009, 2010, and 2011 using Nortek Aquadopp current profilers (2000 kHz frequency). The ADCPs were set up in a bottom-resting, upward-looking configuration at different locations within the Bay (Figure 1b) and programmed to record current data with a bin size of 0.25 m and ensemble lengths of 900 or 1800 s. Deployment locations and additional details are listed in Table 1.

2.1. Lagrangian Drifters

Multiple drifters were deployed between the Saginaw River mouth and Shelter Island (SI in Figure 1b) on 3 days toward the end of July. Deployment dates and start locations are given in Table 2. The drifters were

© 2014. American Geophysical Union. All Rights Reserved.

Table 1. Details of ADCP Deployments in Lake Huron and Saginaw Bay

Deployment Date	Location	Longitude	Latitude	Depth (m)
07/22/09–08/04/09	203	−83.90235	43.673233	3.0
08/04/09–08/18/09	216	−83.897016	43.680066	2.0
08/20/09–09/02/09	232	−83.897016	43.680066	2.9
09/02/09–09/16/09	245	−83.91055	43.699066	3.3
07/13/10–07/27/10	194	−83.917683	43.702916	2.4
07/30/10–08/12/10	211	−83.916666	43.702916	2.5
07/27/11–08/28/11	8119	−83.8525	43.688333	3.6
07/27/11–08/28/11	8126	−83.789166	43.670000	4.0

originally designed by Michael McCormick of the Great Lakes Environmental Research Laboratory (GLERL), Ann Arbor, Michigan. The drifters used in the present study were constructed following the original design using a fiberglass and plywood cross-frame with vinyl drogues (area of 20″ × 35″) to reduce latency as shown in Figure 2. Locations of drifters were tracked in real time using Trackpack® GPS transmitters programed to report location every 30 min. The transmitters were encased in water-resistant housing and the manufacturer-reported uncertainty in GPS location is about 5 m.

2.2. Numerical Model

The three-dimensional unstructured grid numerical model (FVCOM) [*Chen et al*., 2003] is used to describe circulation and thermal structure in Lake Huron and Saginaw Bay. The model solves the hydrodynamic primitive equations using the hydrostatic assumption in the vertical direction with the Boussinesq simplification for convective flows. Vertical eddy viscosity and diffusivity are modeled using the Mellor-Yamada 2.5 level turbulence closure scheme [*Mellor and Yamada*, 1982; *Galperin et al*., 1988]. The horizontal diffusion coefficients are calculated using the Smagorinsky turbulence closure model [*Smagorinsky*, 1963]. Details of the governing equations and boundary conditions can be found elsewhere [e.g., *Chen et al*., 2003].

Two separate hydrodynamic models: (a) the Lake-Wide Model (LWM) and (b) Saginaw Bay Model (SBM) (including the Saginaw River mouth) were setup to resolve large-scale, lake-wide circulation and circulation within the Saginaw Bay, respectively. The grids used in the hydrodynamic models are shown in Figures 3b and 3d. The LWM uses an unstructured grid with 9611 nodes and 17,619 triangular elements in the horizontal (average element size = 2.5 km) and has 21 σ-levels in the vertical. The average resolution at the boundary was about 2.0 km with higher resolution near important features. The SBM uses an unstructured grid with 8236 nodes and 15,575 triangular elements (average element size is approximately 200 m) in the horizontal and 21 σ-levels in the vertical. The minimum element size of 45 m is used near the Saginaw River mouth. Coupling between the LWM and SBM is one-way. Simulated hourly water levels and velocities at the boundary of the SBM, taken from the LWM, were used to drive the SBM. Discharge from the Saginaw River, though considered negligible to LWM circulation and hydrodynamics, was used to provide a flux boundary condition in the SBM. Daily discharge measured at the USGS gaging station on the Saginaw River (04157000) provided the boundary condition at the Saginaw River mouth in the SBM model. The unstructured meshes for LWM and SBM were created using the Surface Water Modeling System (SMS; www.aquaveo.com) and bathymetry at node locations was interpolated from the 6 arc-second bathymetry data downloaded from the NOAA National Geophysical Data Center, Geophysical Data System (GEODAS) website. The LWM computational domain was treated as a closed boundary, and inflow through the Straits of

Table 2. Details of Lagrangian Drifter Deployments in Saginaw Bay

	Deployment Locations			
Day	Longitude	Latitude	Deployment Time	Picking-up Time
Day 1	−83.846734	43.655956	07/27/11 18:44	07/28/11 18:44
	−83.842742	43.661277	07/27/11 18:21	07/28/11 18:51
	−83.839867	43.661309	07/27/11 18:23	07/27/11 23:53
Day 2	−83.840640	43.661288	07/28/11 20:21	07/29/11 18:21
	−83.839266	43.661374	07/28/11 20:23	07/29/11 17:53
Day 3	−83.843365	43.658445	07/29/11 18:44	08/01/11 07:44
	−83.837743	43.662919	07/29/11 19:23	07/30/11 03:53

© 2014. American Geophysical Union. All Rights Reserved.

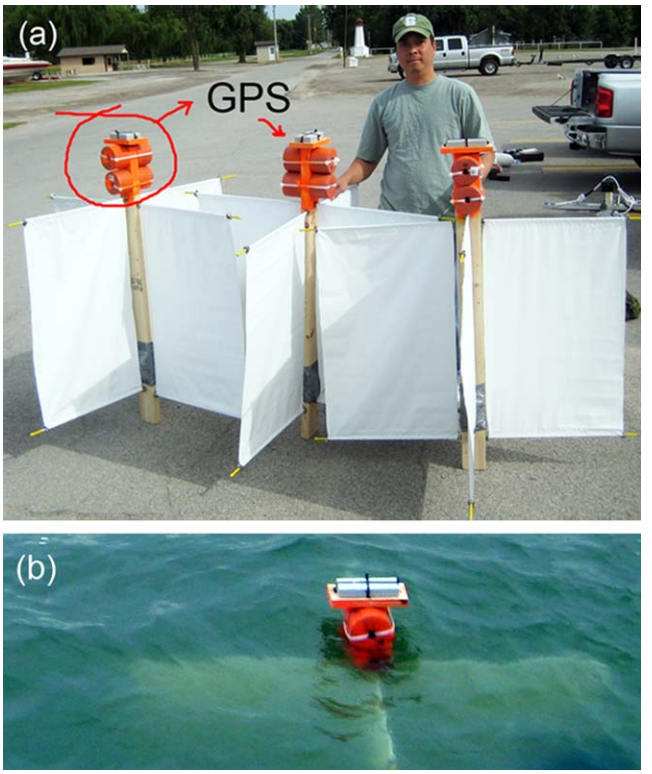

Figure 2. Photographs showing (a) the Lagrangian drifters and (b) a drifter in water (photographs were taken by the last author).

Mackinac, St Mary's River, or other tributaries and outflow to Lake St. Clair via the St. Clair River were not included in the numerical model. The computational meshes used to resolve the hydrodynamics and evolution of thermal structure in Lake Huron and Saginaw Bay are shown in Figure 3.

Hourly standard meteorological data such as wind speed, wind direction, and air temperature for the model simulation periods in 2009, 2010, and 2011 were downloaded from 14 National Data Buoy Center Stations (NDBC) around Lake Huron. In addition, hourly meteorological data from 27 stations were also obtained from the Great Lakes Observation System (GLOS). The quality of meteorological data is controlled by the National Data Buoy Center (NDBC) and the National Climatic Data Center (NCDC). The GLOS, NCDC, and NDBC stations used in this study are shown in Figure 1. The observed meteorological data sets such as wind speed, air temperature, cloud cover, and relative humidity were interpolated to the computational domain using a smoothened nearest neighbor method [*Schwab*, 1999]. Surface heat flux, HFLX, is calculated as

$$HFLX = SW + LW + H_{sensible} + H_{latent} \tag{1}$$

The incoming shortwave radiation was calculated as described by *Bunker* [1976]

$$SW = SW_{clrsky}(1 - kc) \tag{2}$$

where SW_{clrsky} is the clear-sky shortwave radiation, calculated using methods described by *Annear and Wells* [2007]. The cloud cover c is converted from NCDC description and k is an empirical parameter. A value of 0.7 was used for k in this study based on *Schwab* [1999]. The incoming long-wave radiation was calculated following *Parkinson and Washington* [1979]:

$$LW = \sigma T_a^4 \left(1 - 0.261 e^{\left(-7.77\times10^{-4}(273 - T_a)^2\right)}\right)(1 + 0.275c) \tag{3}$$

where σ is the Stefan-Boltzmann constant (5.67×10^{-8} W m^{-2} K^{-4}), T_a is the air temperature, and c is cloud cover. Hourly wind and heat flux values were used to force the hydrodynamic models (LWM and SBM) used in this study. The sensible ($H_{sensible}$) and latent (H_{latent}) heat transfers are calculated at each grid point based on a bulk aerodynamic formulation COARE 2.6 developed by *Fairall et al*. [1996]. Lake-wide summer circulation for 3 years (2009, 2010, and 2011) was simulated using the LWM. In order to avoid problems with initialization of the stratified temperature, the model simulations were started on 1 May with a uniform vertical temperature profile determined from observations at 4 NDBC buoys (45003, 45008, 45137, and 45143).

The recorded GPS locations based on the drifter positions were used to calculate the one-point dispersion statistics in Saginaw Bay near the mouth of the Saginaw River. Using the hydrodynamic results from the

© 2014. American Geophysical Union. All Rights Reserved.

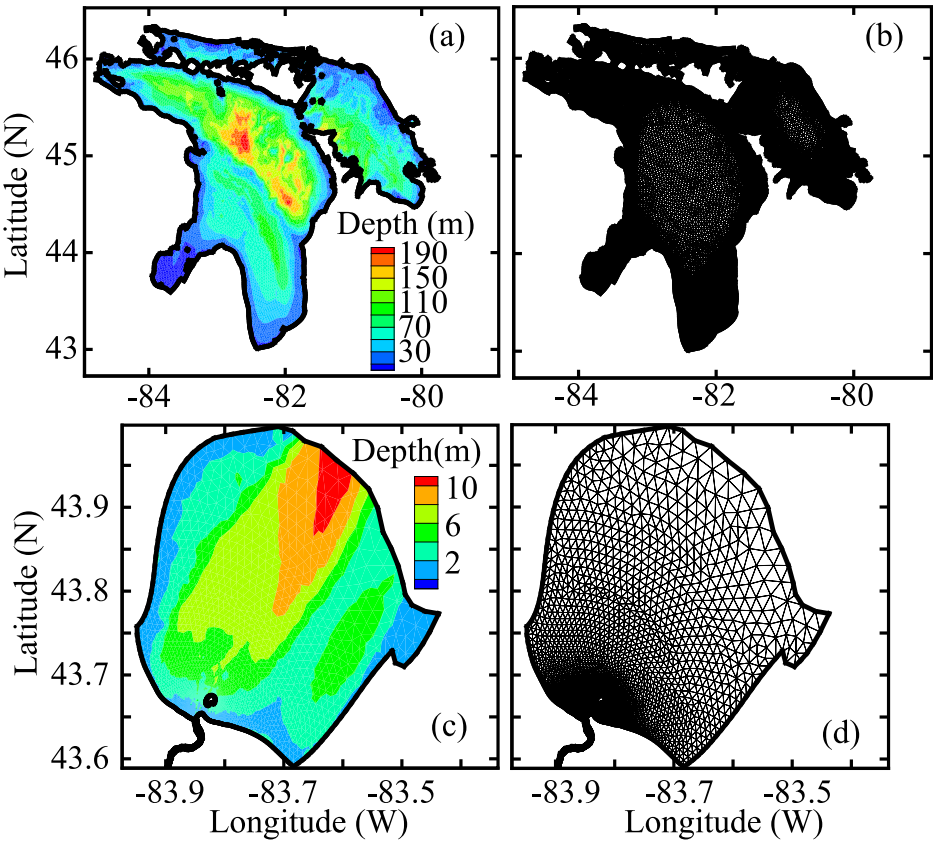

Figure 3. Bathymetry and computational mesh of the (a, b) lake-wide model and (c, d) the Saginaw Bay model.

SBM, a Lagrangian particle-tracking model was used to simulate the drifter trajectories. The simplest case for dispersion in turbulent flow involves the statistical analysis of particles released from a point source in isotropic turbulent flow. Lagrangian statistics provide useful estimates of time and space scales over which flow fields are correlated and are based on the velocity autocorrelation function

$$\rho(\tau)=\frac{\langle u_i(t)u_i(t+\tau)\rangle}{\langle u_i(t)^2\rangle} \tag{4}$$

where $\rho(\tau)$ is the velocity autocorrelation function as a function of the time lag τ, u_i for $i=1,2$ denote the fluctuations in the alongshore and cross-shore components of the velocities (U_i, $i=1,2$) respectively defined as $u_i=U_i-\langle U_i\rangle$, where $\langle U\rangle$ denotes the time-average of the velocity over the period T, where T is the total period of integration. *Taylor* [1921] established that one-particle diffusivity in x direction (κ_{xx}) is related to the derivative of the variance in displacement [*Pope*, 2000]

$$\kappa_{xx}=\frac{1}{2}\frac{d\sigma_{xx}^2(t)}{dt} \tag{5}$$

$$\sigma_{xx}^2=2u'^2\int_0^t(t-\tau)\rho(\tau)d\tau \tag{6}$$

where $u'=\sqrt{\langle U_1^2\rangle}$ is the root mean squared velocity in the x direction and t and τ denote the time and time-lag, respectively, and σ_{xx} is the standard deviation of particle displacements and can be calculated by integrating the Lagrangian autocorrelation (autocovariance) function $\rho(\tau)$. The equation to calculate one-particle diffusivity in the y direction (κ_{yy}) is similar to equation (5). Diffusivity values can be calculated using the zonal and meridional components of the velocity; however, since the Saginaw Bay shoreline is almost

© 2014. American Geophysical Union. All Rights Reserved.

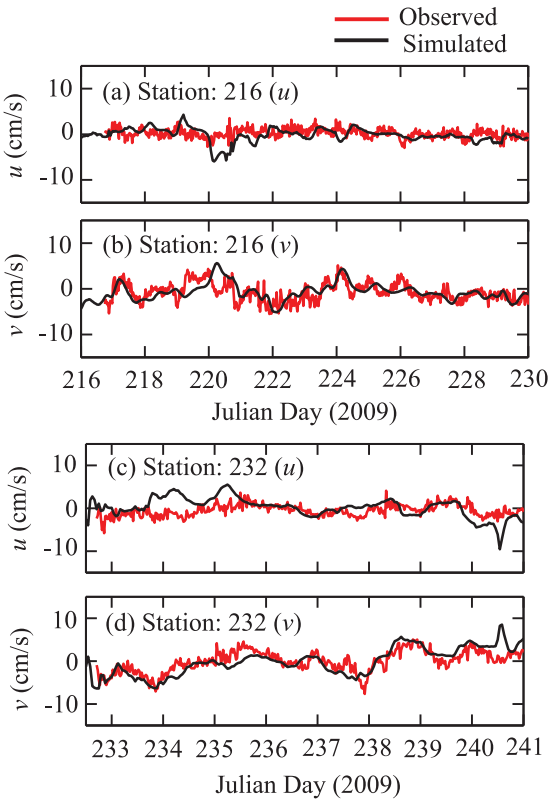

Figure 4. Comparisons between vertically averaged currents from ADCP observations and simulations for the year 2009.

perpendicular to the axis of the bay near the mouth of the Saginaw River where the drifters were released, we used the alongshore and cross-shore velocities to compute the diffusivities in those directions. We used a MATLAB (The Mathworks Inc., Natick, MA, 2013) program based on the `autocorr` function to calculate diffusivity values in the alongshore (x) and cross-shore (y) directions for observed and simulated drifter tracks.

2.3. First-Order Transport Timescales

One of the simplest and most widely used transport timescales is the flushing time (T_f) defined as "the ratio of the mass of a scalar in a reservoir to the rate of renewal of the scalar" [*Geyer*, 1997; *Monsen et al.*, 2002]. Flushing time can be calculated by dividing the volume of the bay (V) by the volumetric flow rate into (Q_{in}) or out of (Q_{out}) the bay (assumed to be equal in this idealized case based on the assumptions of steady state and constant volume). The flushing time as defined here was variously referred to in the past as "residence time" [*Gómez-Gesteira et al.*, 2003; *Chapra*, 2008], "turnover time" [*Sheldon and Alber*, 2006; *Takeoka*, 1984], "flushing time" [*Fischer et al.*, 1979; *Monsen et al.*, 2002; *Delhez et al.*, 2004], "water exchange rate" [*Kraines et al.*, 2001], and "water renewal time" [*Andréfouët et al.*, 2001]. Due to the recirculating nature of the flow within the bay, if we consider a transect separating the bay from the rest of the lake (as shown in Figure 1), then flow enters the bay over a portion of the transect and exits over the remaining portion. The relative extent of these inflow and outflow regions as well as the magnitude and direction of velocities along the transect exhibit unsteadiness throughout the simulation period. These complexities introduce difficulties in the application of the simple flushing time concept. Equation (7) was used to calculate the mean volumetric inflow into Saginaw Bay at the inner (1-1) and outer (2-2) transects shown in Figure 1a to facilitate the application of the flushing time concept. Horizontal velocities from the lake-wide model were interpolated to points on the Saginaw Bay transects and used in equation (7) to calculate the mean inflow (Q_{in}) volume during the summer months. The inflow volumes at the inner and outer transects were used to estimate the flushing rates for the inner and outer bays [*Saylor et al.*, 1976]. The flushing times (T_f) for the inner (and entire) bay are presented in Table 5.

$$\left.\begin{aligned} T_f &= (V/Q_{in}) \\ Q_{in} &= \frac{1}{(t_2-t_1)}\int_{t_1}^{t_2}\left[\int_0^B\left[\int_0^H v_{in}\,dh\right]db\right]dt \\ v_{in} &= \begin{cases} \vec{v}.\hat{n} & \text{if} \quad v.\hat{n} > 0 \\ 0 & \text{if} \quad v.\hat{n} \le 0 \end{cases} \end{aligned}\right\} \tag{7}$$

Here $\vec{v}$ is the velocity (m/s) from the hydrodynamic model, B is the length of the inner (or outer) transect, H is the depth, and t_1, t_2 are the start and end times for the calculations, $\hat{n}$ is a unit vector normal to the transect pointing into the bay (toward southwest), and V is the volume of the inner (or entire) bay.

© 2014. American Geophysical Union. All Rights Reserved.

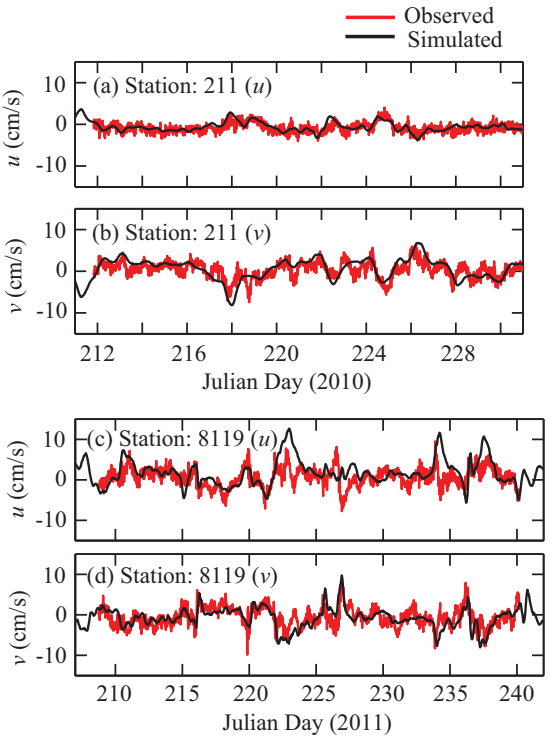

Figure 5. Comparisons between vertically averaged currents from ADCP observations and simulations for years 2010 and 2011.

Another important transport timescale is the residence time (τ_R), which is a measure of "how long a water parcel, starting at a specified location within the water body, will stay within the boundaries of the water body before exiting" [*Monsen et al*., 2002]. By treating the bay as a CSTR (Continuously Stirred Tank Reactor) [*Chapra*, 2008], we can calculate the residence time for every grid cell in the domain as the *e*-folding flushing time [*Monsen et al*., 2002]—that is, the time at which 36.78% (e^{-1}) of the initial mass still remains within the bay. As pointed out by *Monsen et al*. [2002], the flushing time T_f is an integrative system measure while the residence time (τ_R) is a local measure that varies from one grid cell to the other. It is important to recognize that, due to the zero dimensionality and the instantaneous mixing assumptions, the ideal CSTR case does not exactly represent real systems; however, the measures are still useful for understanding and interpreting the behavior of contaminants within the bay. The same hydrodynamic model used for calculating the flushing time T_f was used to calculate the residence time as well (expressed as the *e*-folding flushing time) assuming that the Saginaw Bay was a CSTR. Here it is possible to use different approaches as described in *Burwell et al*. [2000]—a Lagrangian approach in which particles are released and tracked in every grid cell and an Eulerian approach in which the residence time is calculated based on dye concentration modeling. We have used the second approach. In this method, the dye concentration was calculated following the instantaneous dye release at an initial concentration of $C_0 = 100$ ppm in every grid cell in the bay area. The residence time of an element or grid cell is defined as the time it takes for each element's vertically integrated concentration to decrease below 1/e of its initial vertically integrated concentration [*Burwell et al*., 2000]. Since the residence time (τ_R) calculated using this definition would be different for every grid cell, an integrative system measure for the bay ($\bar{\tau}_R$) can be obtained by computing the spatial average of the vertically integrated concentrations for all grid cells in the domain since this average concentration is only a function of time and does not depend on space. The residence time for the bay ($\bar{\tau}_R$) is then calculated as the time it takes for this average vertically integrated concentration in the bay to fall below (1/e) of its initial concentration (i.e., below an average (C/C_0) value of 0.3678). To understand the effect of the Saginaw River on the residence time, we calculate residence times with and without river flow entering the bay. For each case, the hydrodynamic model was run with inflow (or no inflow) from the river and an initial concentration of 100 ppm in every grid cell. For the case with river inflow, the bay was subjected to the initial concentration of 100 ppm, but the river water was assumed to be at a zero concentration; therefore, the residence time estimate for this case represents the effect of flushing of the initial water in the bay by the river. It is important to recognize that flushing time and residence time as calculated here can be expected to yield different estimates of transport timescales since the flushing time concept assumes that advective exchange is the only mechanism of transport while the concentration-based residence time estimate considers the processes of both advection and dispersion in the modeling.

3. Results

As noted by *Beletsky and Schwab* [2001], the spin-up time for the hydrodynamic model was short and the effect of initial conditions on velocity was negligible after about a week of simulation time. Figures 4 and 5

© 2014. American Geophysical Union. All Rights Reserved.

Table 3. RMSE Values and Standard Deviations in Currents Between ADCP Observations and the Results From the Saginaw Bay Model (SBM)

Deployment Date[a]	Location	RMSE (cm/s) (Eastward, Northward Velocity)	Standard Deviations (Eastward, Northward Velocity)	
			Observed	Modeled
08/04/09–08/18/09	216	2.53, 2.68	1.00, 2.00	3.4, 4.7
08/20/09–09/02/09	232	3.82, 3.9	1.49, 2.33	3.51, 4.83
07/13/10–07/27/10	194	3.6, 5.7	1.0, 0.90	2.78, 5.72
07/30/10–08/12/10	211	2.67, 3.09	2.07, 2.89	3.8, 5.2
07/27/11–08/28/11	8119	3.24, 2.23	2.43, 2.36	3.10, 2.47
07/27/11–08/28/11	8126	4.6, 8.9	3.31, 6.36	5.89, 4.17

show typical comparisons between the observed and simulated vertically integrated velocities (east-west velocity *u* and north-south velocity *v*) for all 3 years based on the Saginaw Bay model. The RMSE and standard deviation values for the hydrodynamic model comparisons are summarized in Table 3. The comparisons indicate that model performance was relatively poor for the year 2009. The main reason is due to the missing data for the GLOS stations from May to July in the year 2009 while we started the model at the beginning of May in order to avoid problems with initialization of the stratified temperature. Therefore, the model used only data from the NDBC stations between May and July. This was not an issue for the remaining 2 years (2010 and 2011). In all cases, considering the fact that the ADCPs were deployed in very shallow areas of the bay (2–3 m depth) where the effects from waves and boat traffic are expected to be significant, we conclude that the model was able to describe the vertically averaged velocities reasonably well. The comparisons showed good agreement between the observed and simulated water level fluctuation at station 5035 (Figure 6). In addition to the water levels and the vertically averaged currents, the numerical model was also able to simulate the evolution of temperatures accurately (RMSE values less than 1.7°C) as shown by the comparisons between model results and observations from the ADCPs and data collected at the NDBC buoys presented in Figures 7 and 8, respectively.

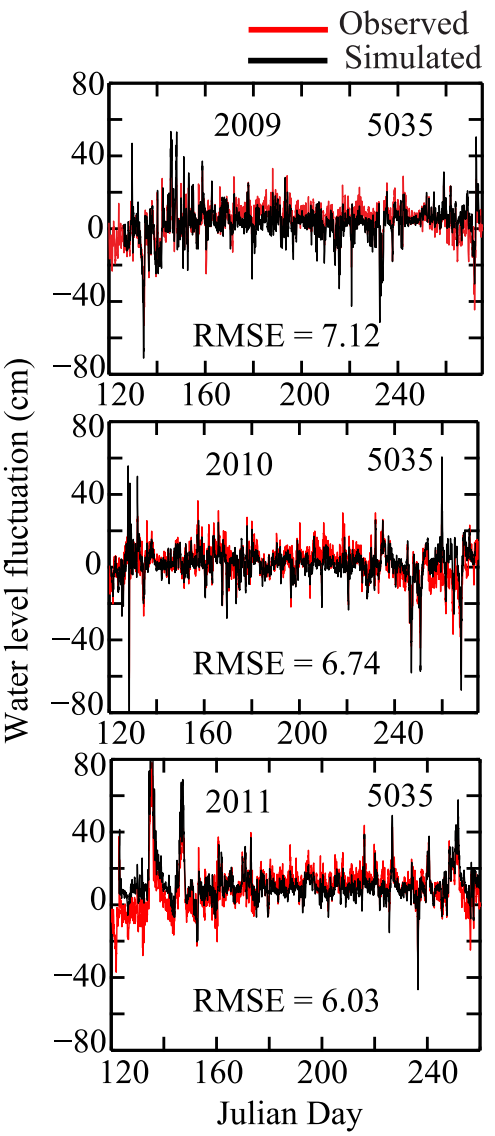

Figure 6. Comparisons between observed and simulated water level fluctuations at station 5035 (Essexville, Michigan) for years 2009, 2010, and 2011.

While comparisons with observations made at a point can be used to quantify model accuracy, dynamic lake-wide processes can be understood by examining the spatial variability in temperatures and currents which are more clearly shown in the vector and contour plots presented in Figures 9–11. Vertically integrated currents based on the original unstructured grid, averaged over each summer month for the 3 year simulation period were interpolated to a uniform Cartesian grid with a step size of 5 km and shown as vector plots in Figure 9. The dominant current patterns are marked using red lines

© 2014. American Geophysical Union. All Rights Reserved.

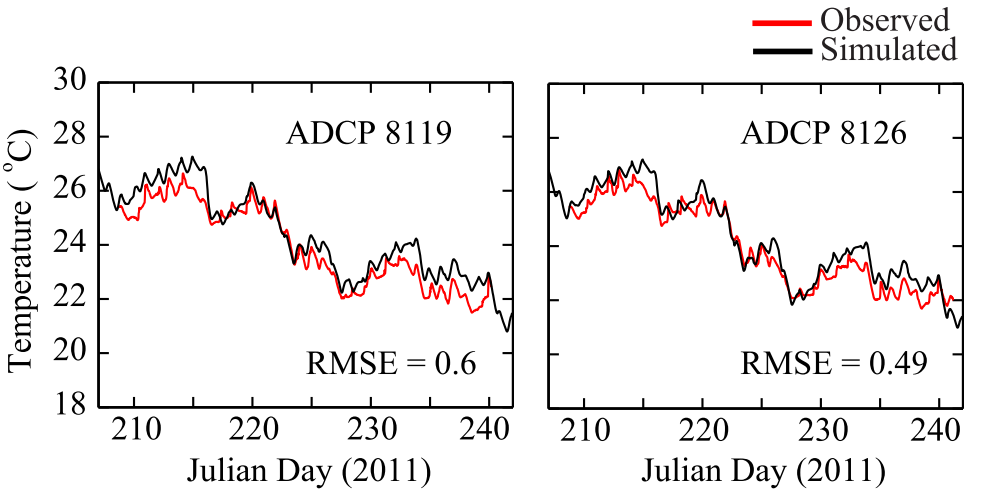

Figure 7. Comparisons between simulated water temperatures and observations from ADCPs for the year 2011.

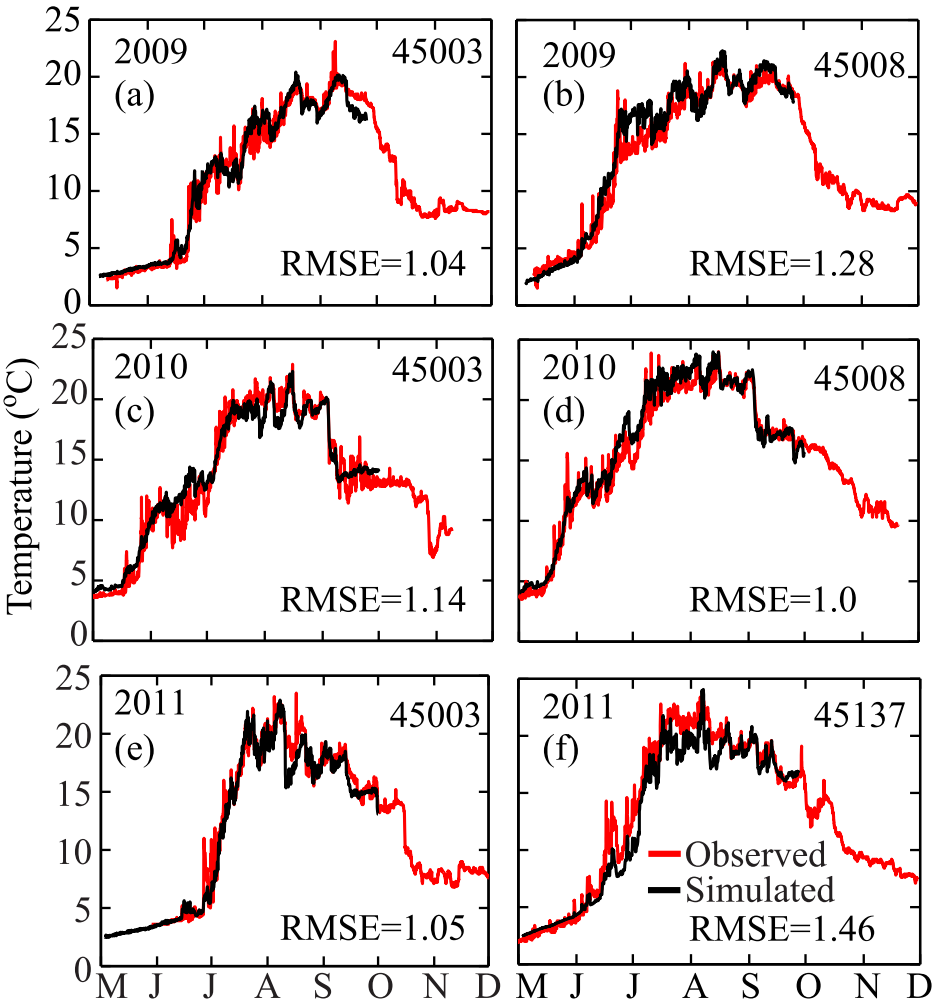

Figure 8. Comparisons between simulated surface temperatures and observations at the NDBC buoys from May to September for the years 2009, 2010, and 2011.

© 2014. American Geophysical Union. All Rights Reserved.

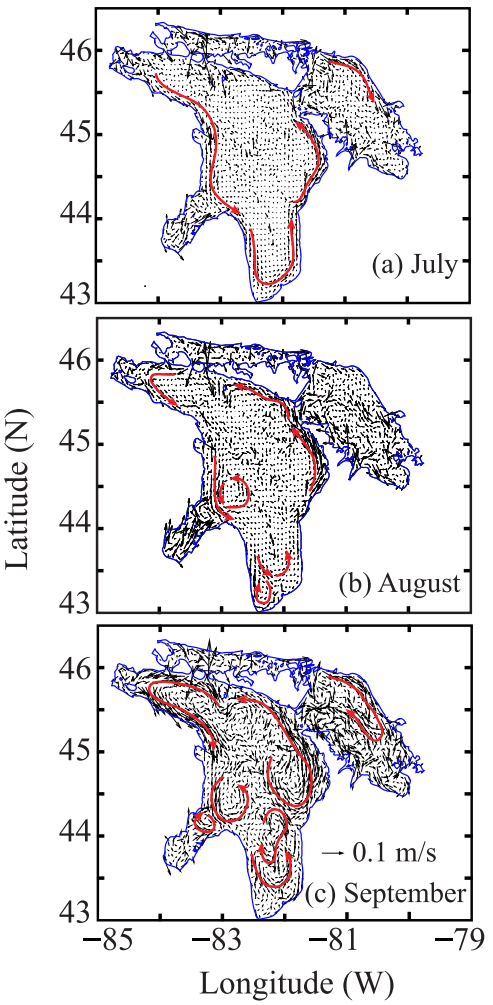

Figure 9. Vertically averaged currents in Lake Huron averaged over the 3 year period (2009–2011) for each summer month (July, August, and September).

with arrows showing the direction of flow. The lake-wide circulation became progressively more pronounced and complex with more gyres appearing as time progressed from July to September while circulation in the Saginaw Bay was strong during the month of August in which the direction of maximum wind velocity (Figure 18) is along the axis of the bay. Details of summer circulation in the Saginaw Bay are shown in Figure 10 by interpolating the vertically integrated currents from the unstructured grid (averaged over the 3 year period) to a uniform Cartesian grid with a resolution of 2 km. We notice the presence of an anticyclonic (that is, clockwise-rotating) gyre at the mouth of the outer Saginaw Bay for all 3 summer months. As noted by others [*Sheng and Rao*, 2006; *Beletsky et al*., 1999], mean circulation in Lake Huron is predominantly cyclonic (counterclockwise) during the summer months (Figure 9). Generally, current speeds are higher closer to the shore and dominated by the alongshore component. Currents in the offshore regions of the lake are smaller and organized into gyres strongly influenced by local topographical features (e.g., MB and the AAR in Figure 1). As expected, vertically averaged currents in the shallower parts of the lake (south and south-west) are higher than values in the deeper parts of the lake (north and north-east). Exchange between Lake Huron and the two main bays (Saginaw Bay and Georgian Bay) is complex and influenced by a number of factors, including topography, stratification, as well as orientation of the shoreline. For example, Figure 12 shows that mean surface flow is into the Georgian Bay and the flow is associated with a return flow in the deeper layers out of Georgian Bay.

As in the other Great Lakes, Lake Huron shows a significant seasonal variation in the thermal structure. The contour plots of surface temperature presented in Figure 11 show the gradual warming of the surface layers as summer progresses. As expected, the shallower parts of the lake warm more quickly and reach the peak of about 25°C in August. However, the shallower Saginaw Bay reaches this value early by July. The dramatic interannual variability in surface temperature is also clear from the results presented in Figure 11, which show the temperature contours for all three summer months and for all three years considered (2009–2011). The vertical variability in temperature is shown more clearly by the temperature profile of the water column along the transects 3-3 and 4-4 in Figures 13 and 14, respectively. The thermal structure of Lake Huron is affected by the central AAR in the main lake as well as the presence of numerous islands. The vertical thermal structure is similar and comparable to previous observations [*Saylor and Miller*, 1979; *Boyce et al*., 1989], and results from numerical simulations in the Great Lakes [*Beletsky and Schwab*, 2001; *Sheng and Rao*, 2006]. We can also see the presence of Ekman flow-driven coastal upwelling in the northeast areas of the lake [*Plattner et al*., 2006] as well as topographically driven upwelling regions associated with sharp changes in bathymetry (e.g., AAR). The impact of these upwelling regions can also be observed in Figure 14 in the form of significantly lower surface water temperatures located north-east of the AAR. These simulated features are also observed in the GLSEA (Great Lakes Surface Environmental Analysis) daily composite temperature images produced from the thermal AVHRR channels of NOAA's polar orbiting weather satellites [*Plattner et al*., 2006; *Leshkevich et al*., 1992].

© 2014. American Geophysical Union. All Rights Reserved.

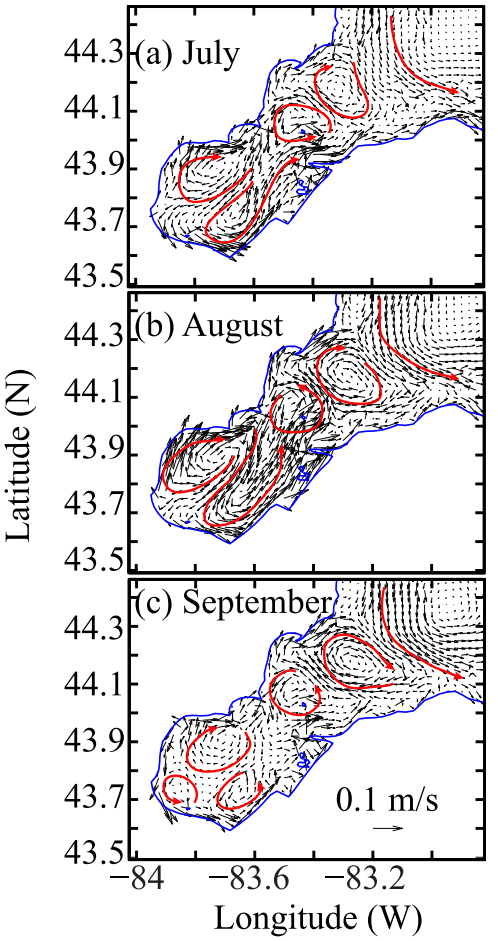

Figure 10. Vertically averaged currents in Saginaw Bay averaged over the 3 year period (2009–2011) for each summer month (July, August, and September).

3.1. Saginaw Bay Model

Results from the high-resolution Saginaw Bay hydrodynamic model (SBM) are presented in Figures 4 and 5. Summary statistics for the comparisons between the ADCP observations and model results are provided as RMSE values in Table 3.

The results from the Lagrangian drifter study and comparisons with observed drifter tracks are presented in Figure 15. As shown by the starting points (initial positions of the drifters at time $t = 0$) marked in the figure, the drifters were released at locations close to the mouth of the Saginaw River where the currents are complex due to plume dynamics and the presence of Shelter Island (SI in Figure 1b). The simulated particle trajectories compare well with GPS locations of the Lagrangian drifters. During the field study, it was observed that the drifters would often get in the shallower depths and get entangled in vegetation present close to the shore in this part of the bay. As a result, mean buoy speeds were used to determine the status of the buoy and comparisons with model are presented only till the first grounding event.

Quality controlled data from the Lagrangian drifters were used to calculate the observed dispersion rates in Saginaw Bay near the Saginaw River plume. Results from the drifter model were used to calculate the model predicted dispersion coefficients. Comparisons between the observed and simulated alongshore and cross-shore dispersion coefficients are shown in Figure 16 for different drifters. Combined wind and wave processes contribute to the observed drifter tracks and dispersion in the field; therefore, some differences can be expected with comparisons based on a purely hydrodynamic model. The comparisons in Figure 16 show that the observed and simulated dispersion coefficients have similar magnitudes and trends. For example, equation (6) predicts a linear spreading rate for short times and square-root spreading for large times. Observed and simulated spreading rates are generally in agreement in describing these limits (Figure 16). Maximum values of dispersion rates based on the comparisons in Figure 16 for drifter 2 are summarized in Table 4.

3.2. Saginaw Bay Exchange Rate

The exchanges between the inner and the outer bays and between the outer bay and the open lake fundamentally control the mean residence time and contaminant flushing rates in Saginaw Bay. The complexity of flows and exchange rates can be seen in Figures 10 and 17, which show the results of vertically averaged currents and surface temperatures in Saginaw Bay for the 3 year simulation period. The presence of two large recirculating cells in the inner bay can be clearly noticed (e.g., in August for all 3 years), and the dominant flow features can be related to the predominant wind patterns shown as wind rose plots in Figure 18 in which the lengths of the histograms denote the frequency of winds coming from a certain direction while the color denotes the magnitude of the wind velocity.

Closer to the mouth of Saginaw River, we also notice the presence of two additional, smaller recirculating cells behind the Shelter Island (not shown in the figures). These flow features, not resolved by the lake-wide model, play an important role in controlling the transport of contaminants in the Saginaw River plume.

© 2014. American Geophysical Union. All Rights Reserved.

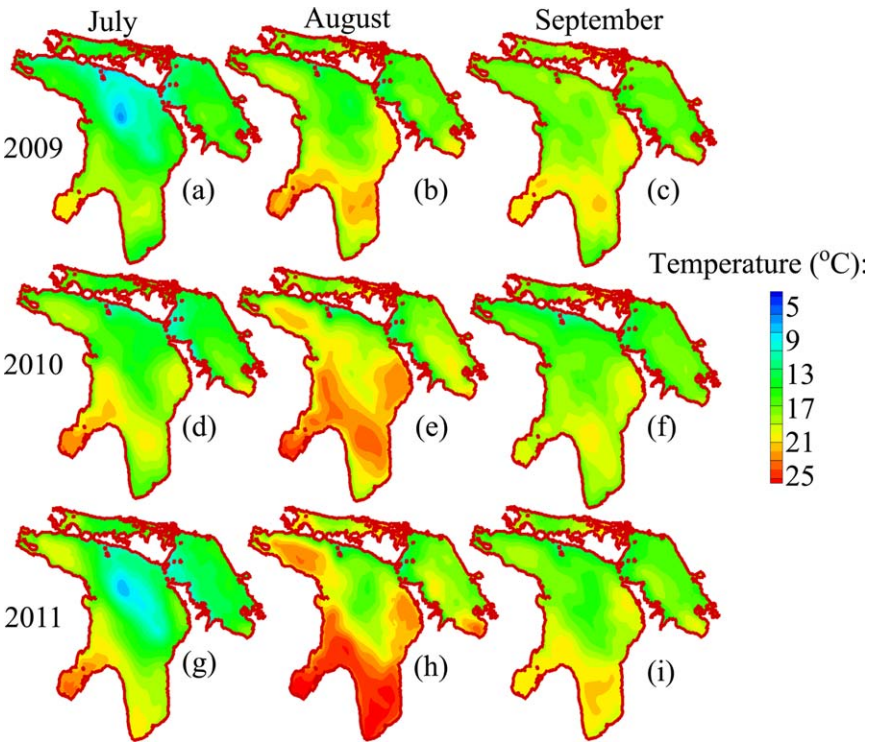

Figure 11. Surface temperature contours for Lake Huron for the summer months July, August, and September in 2009, 2010, and 2011.

Figure 19 shows the vertically averaged volumetric influx as a function of time at the inner (and outer) transects for the summer months of 2009–2011. Exchange at the outer transect 2-2 (Figure 19a) is significantly higher compared to the exchange at the inner transect 1-1. We also notice that the rate of exchange between the inner and outer bays (Figure 19b) shows a significantly larger variation (varies by nearly 4 orders of magnitude) compared to the exchange between the outer bay and the lake (Figure 19a). One of the reasons for this large difference in the variability of exchange rates is the widely different cross-sectional areas at sections 1-1 and 2-2 in Figure 1 as well as the presence of an anticyclonic gyre in the outer bay (shown in Figure 10). The cross-sectional area for the inner bay transect 1-1 is approximately 0.09 km^2 while the area is 1.31 km^2 at the outer transect 2-2.

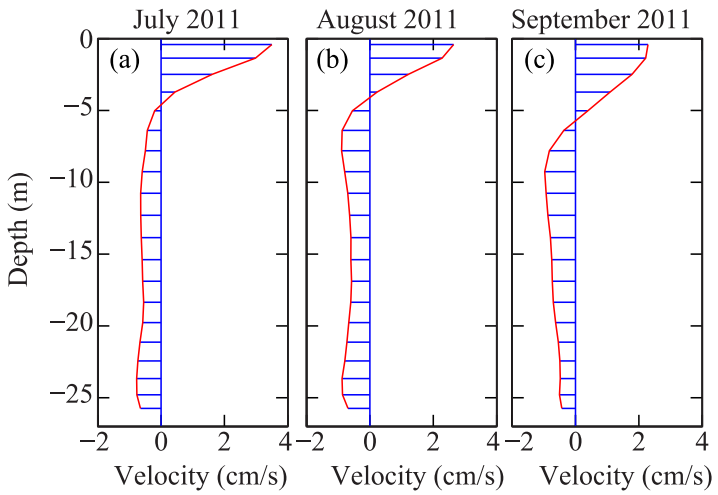

Figure 12. Mean vertical velocity profiles at the inlet of Georgian Bay confirming the return flow suggested by *Beletsky et al.* [1999].

© 2014. American Geophysical Union. All Rights Reserved.

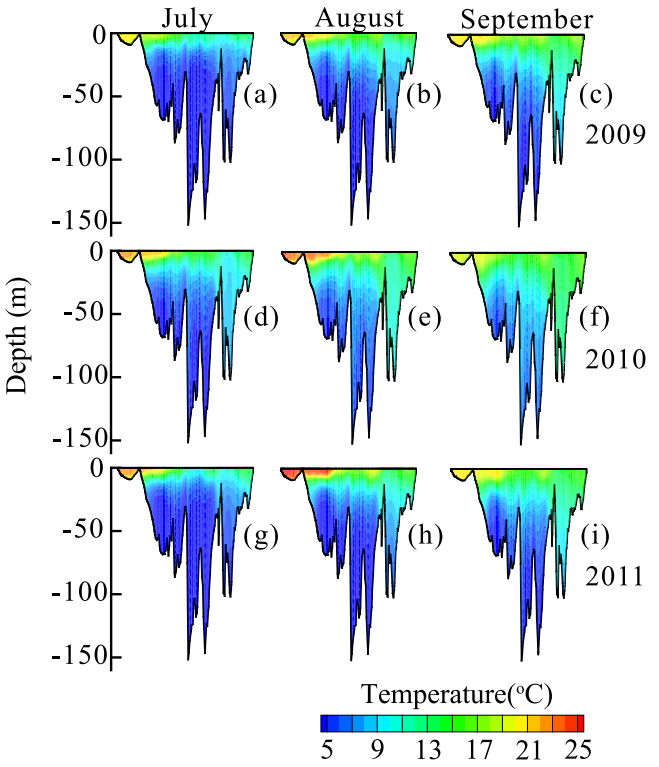

Figure 13. Mean monthly temperature profile along the transect 3-3 in Figure 1.

The Eulerian method is a dye concentration-based modeling, where the bay is initialized with a concentration of 100 ppm under the weather conditions of early May 2011. To understand the spatial variation of residence times within the bay and the effects of Saginaw River inflow on the residence time, we ran the dye transport model for two cases in which dye was released within the inner bay or the entire bay either with or without river inflow. The residence time is defined and calculated as described in section 2. The contour map of residence times in the inner bay and the entire bay with and without river flow and the relationship between the vertically integrated concentration averaged over the entire bay and the residence time are presented in Figures 20 and 21, respectively.

4. Discussion

Large-scale circulation in Lake Huron is influenced its key physical features (several large islands, exchange with Georgian Bay and Saginaw Bay, and the midlake AAR ridge). Field observations and results from numerical models have shown that circulation in the main lake is generally counter clockwise (cyclonic) but not as organized as in Lake Superior due to the presence of the midlake ridge. The lake-wide numerical model was able to simulate this feature during the summer months. The mean current speed was around 3 cm/s while currents as high as 20 cm/s were found in Eastern Georgian Bay. Exchange with Georgian Bay was uniform over the summer months and the mean surface current speed in the channel connecting Georgian Bay with Lake Huron was about 4 cm/s. Surface currents into Georgian Bay during the summer months are associated with a return flow at greater depths as indicated by *Beletsky et al*. [1999]. This feature was confirmed by our numerical model as shown by the vertical profile of mean current velocity at the mouth of Georgian Bay presented in Figure 12. The mean velocity in the deeper layers is about 1 cm/s and generally flows from Georgian Bay into Lake Huron. Here the surface layer coincides with the epilimnion and deeper layer coincides with the hypolimnion. Therefore, it is likely that the direction of flow at a particular depth is influenced by the strength of the stratification and changes from year to year.

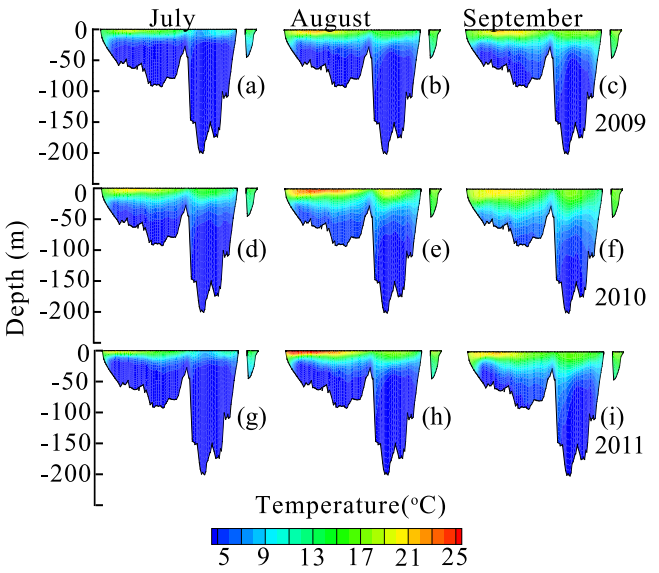

Figure 14. Mean monthly temperature profile along the transect 4-4 in Figure 1.

© 2014. American Geophysical Union. All Rights Reserved.

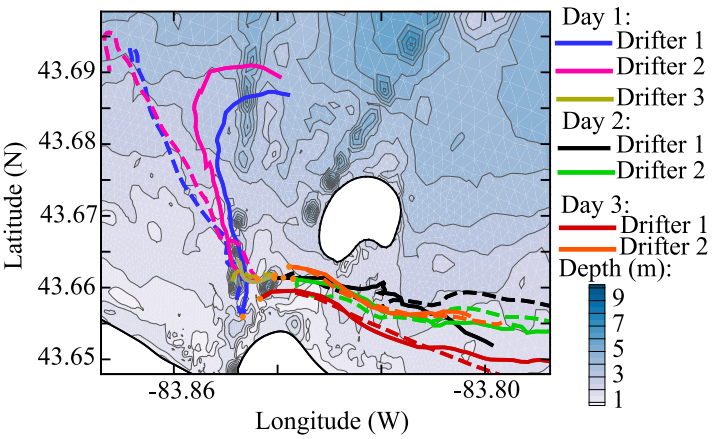

Figure 15. Comparisons between observed positions of GPS-enabled Lagrangian drifters and simulated particle trajectories based on the Saginaw Bay hydrodynamic model. For each drifter, the solid lines (observed) and dashed lines (simulated) are shown in the same color.

Interannual variability of currents was evaluated using mean current speeds for different months. We found that current speeds were highest during the year 2010, with a mean current speed of about 4 cm/s.

As a result of differences in area, volume and size of entrance channel, circulation within Saginaw Bay and Georgian Bay are very different. Mean summer circulation in Georgian Bay was largely counterclockwise with a mean speed of about 3 cm/s. However, circulation in Saginaw Bay was much more complex and depended on the wind direction as noted by *Saylor and Danek* [1976] and *Danek and Saylor* [1977]. The circulation at the entrance of Saginaw Bay was either clockwise (for southwest wind direction) or counterclockwise (for northeast wind direction) depending on the wind direction. Winds blowing perpendicular to the axis of the bay did not significantly affect currents within the bay. Current speeds within Saginaw Bay are generally higher than in the lake resulting in higher mixing due to dispersion. Another important feature of circulation within Saginaw Bay was the difference between hydrodynamics in the inner and outer bays and the effect on exchange between the two. We found that currents along the coast are aligned with the prevailing wind direction. Currents in the central (deeper) part of the bay flow in the opposite direction.

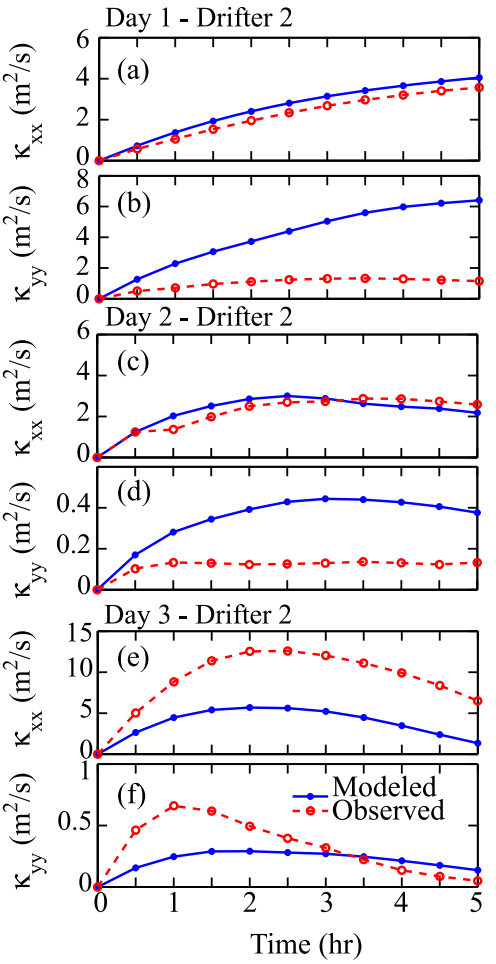

Figure 16. Comparisons between observed and simulated values of single-particle (absolute) horizontal diffusivities in the Saginaw Bay based on data for different drifters.

Similar to other large, deep lakes, the thermal structure in Lake Huron shows significant seasonal variability. The hydrodynamic model simulations were initialized with constant temperature based on the observed water temperature measured at the buoys. As shown by the vertical temperature profiles presented in Figures 13 and 14, the

© 2014. American Geophysical Union. All Rights Reserved.

Table 4. Maximum Values of Absolute Dispersion Rates (in m^2/s) for Lagrangian Drifters and Simulated Particle Paths in Saginaw Bay for Drifter 2

	Cross-shore Diffusivity (κ_{yy})		Alongshore Diffusivity (κ_{xx})	
Day	Observed	Modeled	Observed	Modeled
Day 1	1.33	7.0	3.9	4.1
Day 2	0.16	0.44	2.87	3.1
Day 3	0.66	0.29	12.5	5.7

Table 5. Mean Flushing Time T_f (in Days) for Inner (and Entire) Saginaw Bay

Year	Areas	July	August	September
2009	Inner Bay	23.9	26.2	19.7
	Entire Bay	8.8	13.9	9.1
2010	Inner Bay	26.3	25.0	19.5
	Entire Bay	9.1	8.9	8.6
2011	Inner Bay	25.1	24.4	16.8
	Entire Bay	11.6	10.1	9.2

process of stratification is generally complete by August. The thermocline was located at a depth of about 9 m with an interannual variability of less than 4 m. By including a surface wind-wave mixing scheme, *Bai et al.* [2013] reproduced a reasonable thermal structure with a sharp thermocline located at a depth of

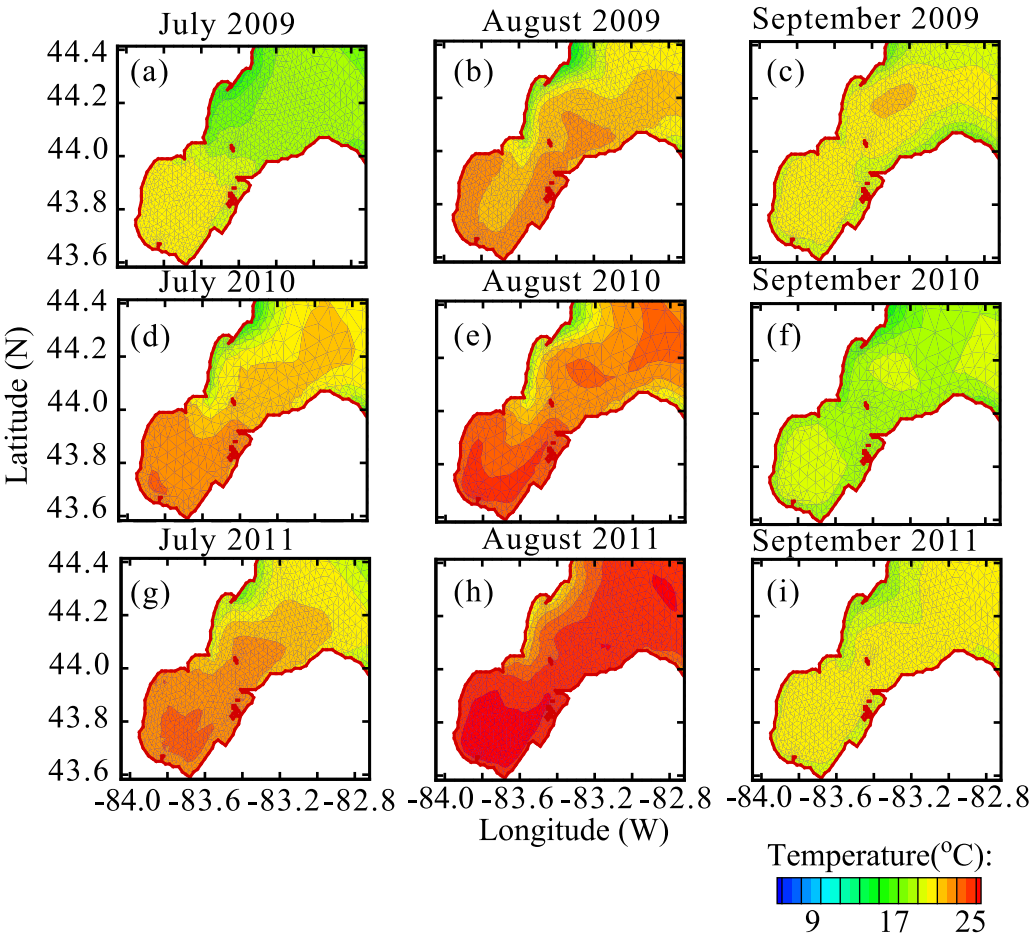

Figure 17. Mean surface temperature contours in Saginaw Bay for July, August, and September in 2009, 2010, and 2011.

© 2014. American Geophysical Union. All Rights Reserved.

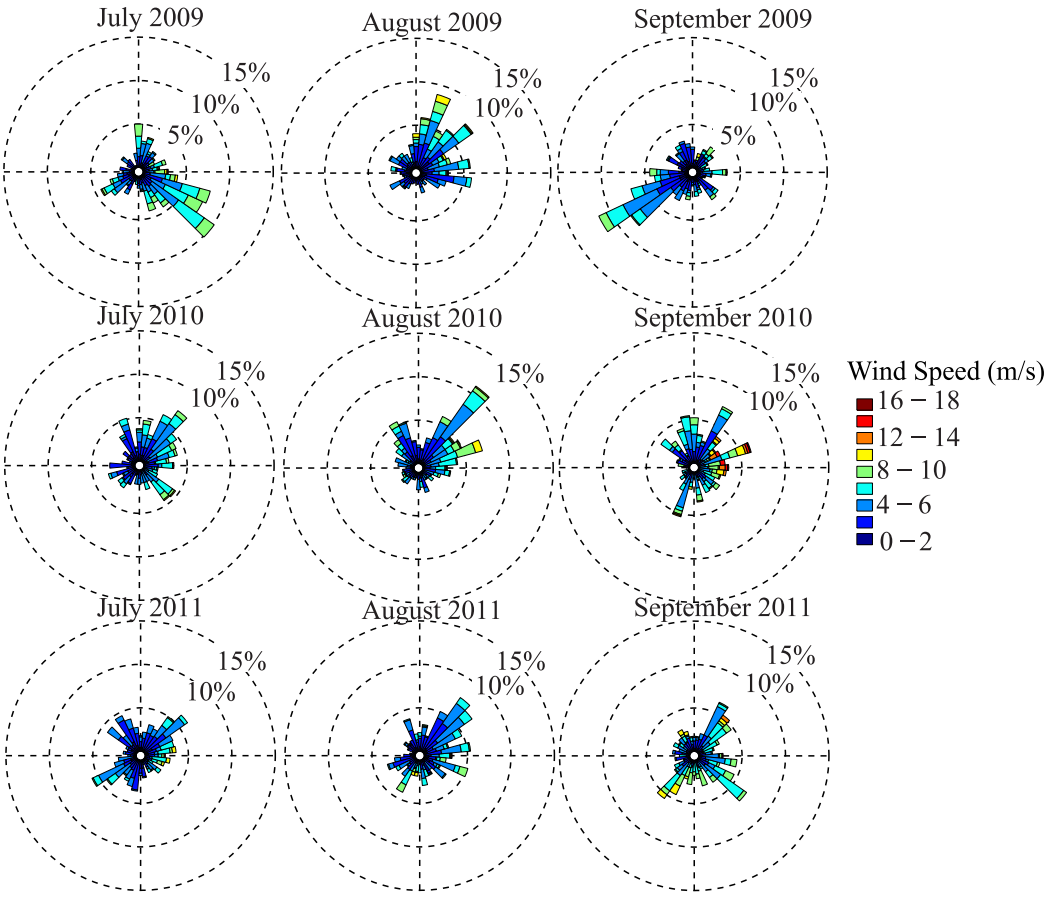

Figure 18. Wind rose plots for summer months during the years 2009–2011.

about 15 m in the Great Lakes in August. Since the hydrodynamic models use the σ–coordinate, we expect a marginally diffused thermocline as noted in *Beletsky and Schwab* [2001]. Due to the lack of any temperature profile measurements in the vertical, a quantitative comparison of the accuracy of the thermal model is not presented; however, comparisons of temperatures in deeper parts of the lake measured by ADCPs are shown in Figure 7 which show a good agreement between observations and the model (RMSE values are less than 0.6°C). As shown in Figure 11, the southern (shallower) part of the lake warms more quickly. However, as shown in Figure 8, surface water temperature in the lake has a high interannual variability, especially in the beginning of summer (June). These variations in monthly mean water temperatures could be due to global climate dynamics. The influence of the midlake ridge on thermal structure in the main lake is also clear from Figure 11. The deepening thermocline reaches the midlake ridge (~20 m) by around August. At this point, exchange between the hypolimnion of the northeastern and southwestern basins is limited and exchange between the two basins is largely in the surface (epilimnion) layers.

Several researchers have observed topography driven upwelling in the marine environment [e.g., *Figueroa and Moffat*, 2000]. However, such features have not been observed in the Great Lakes to the best of our knowledge. Given the highly variable topography in Lake Huron (compared to the other Laurentian Great Lakes), conditions are favorable for the upwelling and hydraulic jumps at several locations in the main lake as well as near Saginaw Bay. Coastal upwelling possibly due to Ekman flow driven by prevailing wind is observed near the northeastern part of the lake. Figure 11 shows the temperature profile along the transect 3-3 marked in Figure 1a. During the stratified summer period, we can see that colder waters are forced upward near the AAR. This indicates the presence of a topographically driven upwelling and possible ventilated thermocline in central Lake Huron. Another region of interest for this study is the sill at the mouth of Saginaw Bay (BCB in Figure 1). Since the depth here is about 15 m and the upper mixed layer reaches the

© 2014. American Geophysical Union. All Rights Reserved.

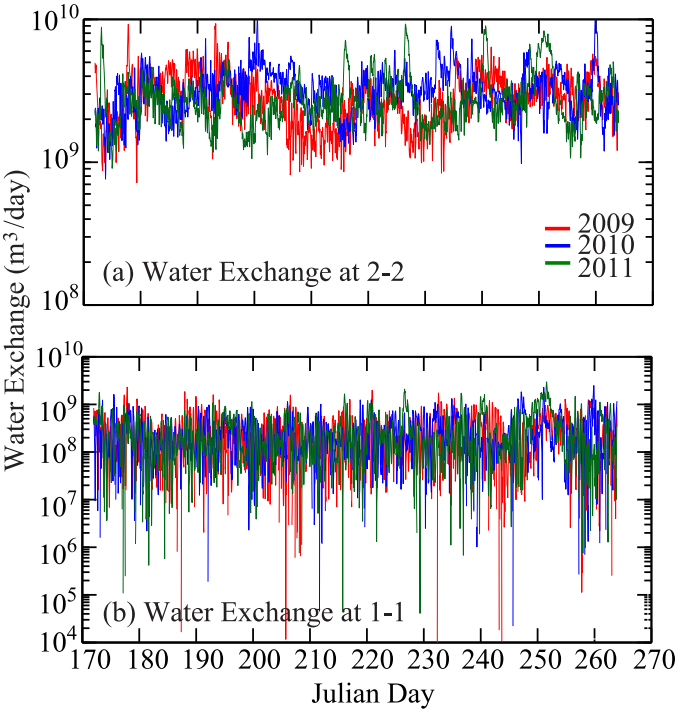

Figure 19. Monthly mean water exchange rates for the inner transect (1-1 in Figure 1) and he outer transect (2-2 in Figure 1) in Saginaw Bay.

lake bottom, no upwelling regions are evident here. However, it is possible that strong currents as a result of winds from the southwest could setup conditions favorable for a hydraulic jump.

The high-resolution Saginaw Bay hydrodynamic model was able to resolve the small-scale bathymetry features and their influence on the circulation within the bay. We used these results to simulate the trajectory of Lagrangian drifters that were released near the mouth of the Saginaw River. As shown in Figure 15, the Lagrangian drifters moved in either an eastward or northward direction after release near the Saginaw River mouth. The general direction of the drifters was affected by the prevailing winds and indicative of the complex plume dynamics near the mouth of a large river. The model was able to predict the general direction of the drifters on all the days as shown in Figure 15. It must be noted that due to the shallow bathymetry and vegetation near the coast in this part of the Saginaw Bay, the drifters would often get grounded. As a result, only short-term comparisons with the Lagrangian drifters are provided here. Long-term drifter trajectories might track the gyres in the inner and outer Saginaw Bay that are predicted by the numerical model.

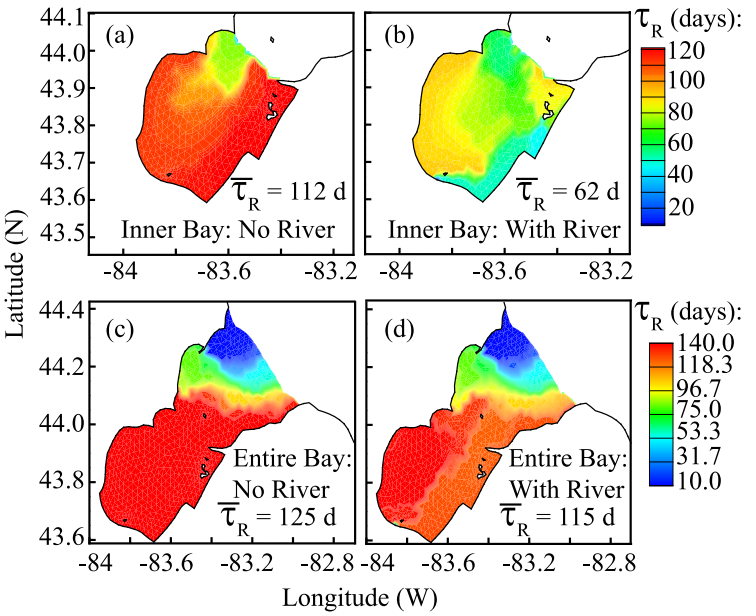

Figure 20. Contour plots of residence time (in days) for Saginaw Bay based on dye concentration modeling. Figures 20a and 20b are for inner bay dye releases with (a) no river inflow and (b) with river inflow. Figures 20c and 20d are the results based on dye releases for the entire bay with (c) no river flow and (d) with river flow.

© 2014. American Geophysical Union. All Rights Reserved.

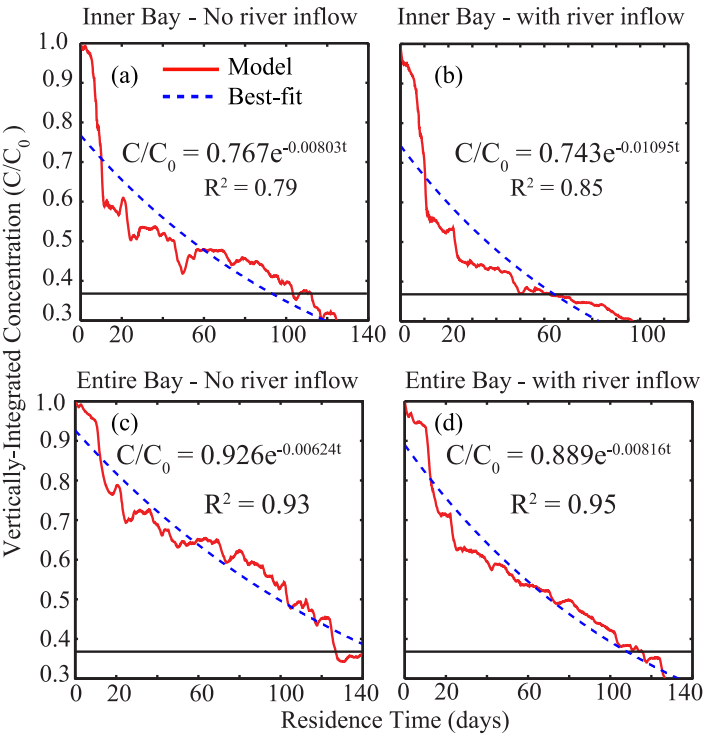

Figure 21. Average vertically integrated concentration in the Saginaw Bay as a function of time. The red solid lines represent the model results while the blue dashed lines represent an exponential decay model fit to the data. The concentration value corresponding to a value of (1/*e*) is also marked.

Data from the Lagrangian drifter study were also used to calculate the absolute dispersion rates near the mouth of Saginaw River. Figure 16 shows a comparison of the model derived Lagrangian single-point (absolute) dispersion rates in the alongshore and cross-shore directions (κ_{xx}, κ_{yy}) with observed values. It is clear from the observed values that dispersion is (a) highly anisotropic and (b) variable with time. The model is able to predict some of this variability. However, with time the difference between observed and simulated values increases.

The mean residence time for contaminants entering the Saginaw Bay from point and nonpoint sources in the bay was estimated from two different methods. The first method used results from the lake-wide numerical model. The flushing rates for water (and dissolved contaminants) in the inner and outer bay were calculated using equation (7) for different months during 2009–2011 are presented in Table 5. The mean flushing time for all three summers (and all 3 years) was 23.0 days for the inner bay and 9.9 days for the entire bay. In an earlier study, *Saylor and Danek* [1976] estimated a mean flushing time of 26.5 days for the inner bay. This difference is explained by the change in volume of the inner bay (from 8.5 km^3 in 1976 to 6.5 km^3 in 2012) over the past four decades due to falling lake levels. The results presented in Table 5 clearly show that flushing rate for the outer bay is almost twice as much as for the inner bay. This could be due to the role played by lake-wide circulation on flow in the outer bay. Currents within the Saginaw Bay are strongly affected by the direction of wind. Wind blowing out of the southwest or northeast is associated with higher mean current speeds and, therefore, greater mixing and dilution as well as a smaller mean residence time. No such trend is apparent for the mean flushing rate for the outer bay, which is affected to a

Table 6. Mean Residence Time (*e*-Folding Flushing Time) in Days for Inner and Outer Saginaw Bay

		Case	
Year	Areas	No River Inflow	With River Inflow
2011	Inner Bay	112	62
	Entire Bay	125	115

© 2014. American Geophysical Union. All Rights Reserved.

greater degree by the large-scale circulation. Using an Eulerian dye concentration-based approach, we calculated the mean residence time (*e*-folding flushing time) in the bay as described earlier. The residence time results are shown in Table 6. The range of values is from 62 to 125 days depending on whether inflow from the Saginaw River is considered or not. An earlier study by *Dolan* [1975] calculated a residence time of 110 days for the inner bay and 52 days for the entire bay based on a time-variable chloride model. Their results, based on "well-mixed" mass balance models [*Chapra*, 2008], allow the bay to be divided into a few (e.g., three) segments taking both advective and dispersive exchange across segments into account. Since the present work is based on fully three-dimensional hydrodynamic and transport models, our residence time estimates can be expected to differ from those of *Dolan* [1975]. The results presented in Table 6 show that residence times calculated by the Eulerian dye concentration-based model are greater than the mean flushing times calculated using the first method which considers only advective exchange. This difference can be explained by the increased time due to mixing and dilution in the entire bay. The low residence times occur in the middle of the bay, and high residence times along the shoreline and the Saginaw river mouth areas (Figure 20). For the case of dye release into the entire bay, low residence times were found in the areas near the mouth of the Saginaw Bay (5–50 days) while the remaining areas have relatively high residence times (more than 140 days; Figure 20). The figure clearly shows the important role played by the gyres near the mouth of the outer Saginaw Bay on residence times. As can be seen from Figure 20, river inflow has a significant effect on the residence time of the inner bay although the effect is almost insignificant when the entire bay is considered (Figure 20d). This is not surprising since the inner bay is fairly shallow and is readily influenced by riverine discharge while the gyres and the larger lake-wide circulation mainly influence the outer bay residence time. Figure 21 shows the vertically integrated concentrations within the bay (averaged over the spatial extent of the bay) as a function of time for the different cases considered (inner bay and entire bay with and without river flow). The figure shows the model results and the best exponential fit to the model results. Generally, the declining concentrations follow an exponential curve with R^2 values ranging from 0.79 to 0.95.

5. Conclusions

The mean summer circulation in Lake Huron and Saginaw bay was examined using an unstructured grid hydrodynamic model based on the FVCOM. The model was tested using ADCP observations in Saginaw Bay, surface temperature measurements at NDBC buoys, and Lagrangian drifter trajectories. Using the unstructured grid model we were able to simulate the small-scale features in Saginaw Bay and Georgian Bay as well as lake-wide circulation in Lake Huron. The hydrodynamic model was able to reproduce the anticyclonic (counterclockwise) lake-wide circulation patterns that have been observed in earlier numerical and field studies on Lake Huron. We found that mean current speeds close to the shore can be as high as 20 cm/s compared with the lake-wide average of 3 cm/s. The complex topography coupled with stratification and rapid warming of the southern part of the lake results in high interannual variability in surface temperature values. Several potential upwelling regions have been identified where topographically driven upwelling brings cold water from the deeper layers to the surface. One such region is in the strait connecting Lake Huron with Georgian Bay. In addition to upwelling, our simulations show that in the surface layer (epilimnion) mean flow during summer is from Lake Huron into Georgian Bay, which sets up a return flow in the deeper layers (hypolimnion) from the bay into the lake. Since the hypolimnion is 3–4 times thicker than the epilimnion in this part of the lake, surface velocities are several times larger in magnitude than the velocities in the deeper layers.

Results from the Lagrangian drifter study in Saginaw Bay showed the highly anisotropic and time-variable nature of dispersion near the mouth of the Saginaw River with the alongshore diffusivities being typically greater than the cross-shore values. The numerical model was able to predict the drifter trajectories and dispersion coefficients reasonably well. However, differences between observed and predicted values increased with time.

Water mass exchange rates for Saginaw Bay were calculated using results from the numerical model. The influx rates (m^3/s) at two transects (1-1 and 2-2 in Figure 1) across Saginaw Bay were used to estimate the mean flushing times for the inner and outer Saginaw Bay. The mean flushing time for the inner bay (~23.0 days) was approximately twice that for the entire bay (~9.9 days). This difference is explained by the

© 2014. American Geophysical Union. All Rights Reserved.

topographical features (sill) and the gyres that limit exchange in the inner bay and the large-scale circulation features that increase the exchange rate for the entire bay. Comparing our results with earlier studies [*Saylor et al*., 1976] on the exchange rate for Saginaw Bay, we found that the difference is explained by the change in volume of the inner bay in the last four decades due to falling lake levels. The mean *e*-folding flushing time was found to be 62 days (2 months) for the inner bay and 115 days (3.7 months) for the entire bay.

Acknowledgment
This research was funded by the NOAA Center of Excellence for Great Lakes and Human health.

References

Allender, J. H. (1975), Numerical simulation of circulation and advection-diffusion processes in Saginaw Bay, Michigan, PhD dissertation, Univ. of Mich., Ann Arbor.
Allender, J. H., and A. W. Green (1976), Free mode coupling of Saginaw Bay and Lake Huron, *J. Great Lakes Res.*, *2*(1), 1–6.
Anderson, E. J., and D. J. Schwab (2013), Predicting the oscillating bi-directional exchange flow in the Straits of Mackinac, *J. Great Lakes Res.*, *39*(4), 9.
Andradóttir, H. Ó., F. J. Rueda, J. Armengol, and R. Marcé (2012), Characterization of residence time variability in a managed monomictic reservoir, *Water Resour. Res.*, *48*, W11505, doi:10.1029/2012WR012069.
Andréfouët, S., J. Pages, and B. Tartinville (2001), Water renewal time for classification of atoll lagoons in the Tuamotu Archipelago (French Polynesia), *Coral reefs*, *20*(4), 399–408.
Andutta, F. P., P. V. Ridd, and E. Wolanski (2013), The age and the flushing time of the Great Barrier Reef waters, *Cont. Shelf Res.*, *53*, 11–19.
Annear, R. L., and S. A. Wells (2007), A comparison of five models for estimating clear-sky solar radiation, *Water Resour. Res.*, *43*, W10415, doi:10.1029/2006WR005055.
Bai, X., J. Wang, D. J. Schwab, Y. Yang, L. Luo, G. A. Leshkevich, and S. Liu (2013), Modeling 1993–2008 climatology of seasonal general circulation and thermal structure in the Great Lakes using FVCOM, *Ocean Modell.*, *65*, 40–63, doi:10.1016/j.ocemod.2013.02.003.
Beletsky, D., J. H. Saylor, and D. J. Schwab (1999), Mean circulation in the Great Lakes, *J. Great Lakes Res.*, *25*, 78–93.
Beletsky, D., and D. J. Schwab (2001), Modeling circulation and thermal structure in Lake Michigan: Annual cycle and interannual variability, *J. Geophys. Res. Oceans*, *106*(C9), 19745–19771.
Bolin, B., and H. Rodhe (1973), A note on the concepts of age distribution and transit time in natural reservoirs, *Tellus*, *25*(1), 58–62.
Boyce, F. M., M. A. Donelan, P. F. Hamblin, C. Murthy, and T. Simons (1989), Thermal structure and circulation in the Great Lakes, *Atmos. Ocean*, *27*, 607–642.
Brown, J., J. MacMahan, and A. Reniers (2009), Surf zone diffusivity on a rip-channeled beach, *J. Geophys. Res.*, *114*, C11015, doi:10.1029/2008JC005158.
Bunker, A. F. (1976), Computations of surface energy flux and annual air-sea interaction cycles of the North Atlantic ocean, *Mon. Weather Rev.*, *104*, 1122–1140.
Burwell, D., M. Vincent, M. Luther, and B. Galperin (2000), Modeling residence times: Eulerian versus Lagrangian, in *Estuarine and Coastal Modeling*, edited by M. L. Spaulding and H. L. Butler, pp. 995–1009, Am. Soc. of Civ. Eng., Reston, Va.
Camacho, R. A., and J. L. Martin (2012), Hydrodynamic modeling of first-order transport timescales in the St. Louis Bay Estuary, Mississippi, *J. Environ. Eng.*, *139*(3), 317–331.
Chapra, S. C. (2008), *Surface Water-Quality Modeling*, Waveland Press, Long Grove, Ill.
Chen, C., H. Liu, and R. C. Beardsley (2003), An unstructured, finite-volume, three-dimensional, primitive equation ocean model: Application to coastal ocean and estuaries, *J. Atmos. Oceanic Technol.*, *20*, 159–186.
Danek, L. J., and J. H. Saylor (1977), Measurements of the summer currents in Saginaw Bay, Michigan, *J. Great Lakes Res.*, *3*(1), 65–71.
Delhez, E. J. M., G. Lacroix, and E. Deleersnijder (2004b), The age as a diagnostic of the dynamics of marine ecosystem models, *Ocean Dyn.*, *54*, 221–231.
Dolan, D. M. (1975), Saginaw Bay residence time, internal working paper, U.S. Environ. Prot. Agency, Grosse Ile, Mich.
Fairall, C. W., E. F. Bradley, D. P. Rogers, J. B. Edson, and G. S. Young (1996), Bulk parameterization of air-sea fluxes for tropical ocean-global atmosphere coupled-ocean atmosphere response experiment, *J. Geophys. Res. Oceans*, *101*(C2), 3747–3764.
Figueroa, D., and C. Moffat (2000), On the influence of topography in the induction of coastal upwelling along the Chilean coast, *Geophys. Res. Lett.*, *27*(23), 3905–3908.
Fischer, H. B., E. J. List, R. C. Y. Koh, J. Imberger, and N. H. Brooks (1979), *Mixing in Inland and Coastal Waters*, 483 p., Academic, New York.
Galperin, B., L. H. Kantha, S. Hassid, and A. Rosati (1988), A quasi-equilibrium turbulent energy model for geophysical flows, *J. Atmos. Sci.*, *45*(1), 55–62.
Ge, Z., R. L. Whitman, M. B. Nevers, M. S. Phanikumar, and M. N. Byappanahalli (2012), Nearshore hydrodynamics as loading and forcing factors for *Escherichia coli* contamination at an embayed beach, *Limnol. Oceanogr. Methods*, *57*(1), 362–381, doi:10.4319/lo.2012.57.1.0362.
Geyer, W. R. (1997), Influence of wind on dynamics and flushing of shallow estuaries, *Estuarine Coastal Shelf Sci.*, *44*(6), 713–722.
GoÇmez-Gesteira, M., M. de Castro, and R. Prego (2003), Dependence of the water residence time in Ria of Pontevedra (NW Spain) on the seawater inflow and the river discharge, *Estuarine Coastal Shelf Sci.*, *58*, 567–573.
Harrington, M. W. (1894), *Currents of the Great Lakes as Deduced From the Movements of Bottle Papers During the Seasons of 1892 and 1893*, U.S. Weather Bur., Washington, D. C.
Hsu, K., M. T. Stacey, and R. C. Holleman (2013), Exchange between an estuary and an intertidal marsh and slough, *Estuaries Coasts*, *36*, 1137–1149, doi:10.1007/s12237-013-9631-2.
Jouon, A., P. Douillet, S. Ouillon, and P. Fraunié (2006), Calculations of hydrodynamic time parameters in a semi-opened coastal zone using a 3D hydrodynamic model, *Cont. Shelf Res.*, *26*(12), 1395–1415.
Kraines, S. B., M. Isobe, and H. Komiyama (2001), Seasonal variations in the exchange of water and waterborne particles at Majuro Atoll, the Republic of the Marshall Islands, *Coral Reefs*, *20*(4), 330–340.
Lawrence, G. A., K. I. Ashley, N. Yonemitsu, and J. R. Ellis (1995), Natural dispersion in a small lake, *Limnol. Oceanogr.*, *40*(8), 1519–1526.
Leshkevich, G. A., D. J. Schwab, and G. C. Muhr (1992), Satellite environmental monitoring of the Great Lakes: A review of NOAA's Great Lakes CoastWatch program, *Photogramm. Eng. Remote Sens.*, *59*, 371–379.
Liu, Z., H. Wang, X. Guo, Q. Wang, and H. Gao (2012), The age of Yellow River water in the Bohai Sea, *J. Geophys. Res.*, *117*, C11006, doi:10.1029/2012JC008263.

© 2014. American Geophysical Union. All Rights Reserved.

Mellor, G. L., and T. Yamada (1982), Development of a turbulence closure model for geophysical fluid problems, *Rev. Geophys.*, *20*, 851–875.
Monsen, N. E., J. E. Cloern, L. V. Lucas, and S. G. Monismith (2002), A comment on the use of flushing time, residence time, and age as transport time scales, *Limnol. Oceanogr.*, *47*(5), 1545–1553.
Nekouee, N. (2010), Dynamics and numerical modeling of River Plumes in Lakes, *NOAA Tech. Memo. GLERL-151*, Great Lakes Environ. Res. Lab, Ann Arbor, Mich.
Nixon, S. W., et al. (1996), The fate of nitrogen and phosphorus at the land-sea margin of the North Atlantic Ocean, *Biogeochemistry*, *35*, 141–180.
Ojo, T. O., J. S. Bonner, and C. Page (2006), Observations of shear-augmented diffusion processes and evaluation of effective diffusivity from current measurements in Corpus Christi Bay, *Cont. Shelf Res.*, *26*(6), 788–803.
Okubo, A. (1971), Oceanic diffusion diagram, *Deep Sea Res. Oceanogr. Abstr.*, *18*, 789–902.
Parkinson, C. L., and W. M. Washington (1979), A large-scale numerical model of sea ice, *J. Geophys. Res.*, *84*, 311–337.
Peeters, F., A. Wüest, G. Piepke, and D. M. Imboden (1996), Horizontal mixing in lakes, *J. Geophys. Res.*, *101*, 18.
Phelps, J. J., J. A. Polton, A. J. Souza, and L. A. Robinson (2013), Hydrodynamic timescales in a hyper-tidal region of freshwater influence, *Cont. Shelf Res.*, *63*, 13–22.
Plattner, S., D. M. Mason, G. A. Leshkevich, D. J. Schwab, and E. S. Rutherford (2006), Classifying and forecasting coastal upwellings in Lake Michigan using satellite derived temperature images and buoy data, *J. Great Lakes Res.*, *32*(1), 63–76.
Pope, S. B. (2000), *Turbulent Flows*, 806 p., Cambridge Univ. Press, New York.
Saylor, J. H., and L. J. Danek (1976), Wind-driven circulation of Saginaw Bay, in *15th Proceedings of Coastal Engineering Conference*, pp. 3262–3275, Am. Soc. Civ. Eng., New York.
Saylor, J. H., and G. S. Miller (1979), Lake Huron winter circulation, *J. Geophys. Res.*, *84*, 3237–3252.
Schertzer, W. M., R. A. Assel, D. Beletsky, T. E. Croley II, B. M. Lofgren, J. H. Saylor, and D. J. Schwab (2008), Lake Huron climatology, interlake exchange and mean circulation, *Aquat. Ecosyst. Health Manage.*, *11*(2), 144–152.
Schwab, D. J. (1999), Lake Michigan Mass Balance Study: Hydrodynamic Modeling Project, *NOAA Technical Memorandum ERL GLERL-108*.
Sheldon, J. E., and M. Alber (2006), The calculation of estuarine turnover times using freshwater fraction and tidal prism models: A critical evaluation, *Estuaries Coasts*, *29*(1), 133–146.
Sheng, J., and Y. R. Rao (2006), Circulation and thermal structure in Lake Huron and Georgian Bay: Application of a nested-grid hydrodynamic model, *Cont. Shelf Res.*, *26*, 1496–1518.
Sheng, J., D. G. Wright, R. J. Greatbatch, and D. E. Dietrich (1998), CANDIE: A new version of the DieCAST ocean circulation model, *J. Atmos. Oceanic Technol.*, *15*(6).
Sloss, P. W., and J. H. Saylor (1976), Large-scale current measurements in Lake Huron, *J. Geophys. Res.*, *81*, 3069–3078.
Smagorinsky, J. (1963), General circulation experiments with the primitive equations: I. The basic experiment, *Monthly Weather Review*, *91*(3), 99–164.
Spydell, M., F. Feddersen, R. T. Guza, and W. E. Schmidt (2007), Observing surf-zone dispersion with drifters, *J. Phys. Oceanogr.*, *37*(12), 2920–2939.
Spydell, M. S., F. Feddersen, and R. T. Guza (2009), Observations of drifter dispersion in the surfzone: The effect of sheared alongshore currents, *J. Geophys. Res.*, *114*, C07028, doi:10.1029/2009JC005328.
Stocker, R., and J. Imberger (2003), Horizontal transport and dispersion in the surface layer of a medium-sized lake, *Limnol. Oceanogr. Methods*, *48*(3), 971–982.
Takeoka, H. (1984), Fundamental concepts of exchange and transport time scales in a coastal sea, *Cont. Shelf Res.*, *3*, 311–326.
Taylor, G. I. (1921), Diffusion by continuous movements, *Proc. London Math. Soc.*, *20*, 196–212.
Thupaki, P., M. S. Phanikumar, D. Beletsky, D. J. Schwab, M. B. Nevers, and R. L. Whitman (2010), Budget analysis of *Escherichia coli* at a southern Lake Michigan beach, *Environ. Sci. Technol.*, *44*(3), 1010–1016.
Thupaki, P., M. S. Phanikumar, and R. L. Whitman (2013), Solute dispersion in the coastal boundary layer of southern Lake Michigan, *J. Geophys. Res. Oceans*, *118*, 1606–1617, doi:10.1002/jgrc.20136.
Wan, Y., C. Qiu, P. Doering, M. Ashton, D. Sun, and T. Coley (2013), Modeling residence time with a three-dimensional hydrodynamic model: Linkage with chlorophyll a in a subtropical estuary, *Ecol. Modell.*, *268*, 93–102.

© 2014. American Geophysical Union. All Rights Reserved.